

Synthesis and Characterization of Surfactant (PVP) Capped Zinc Oxide Nanorods

S. Renuka¹, K. Dhanaraj², S.H. Socrates³ and B.Gokulakumar⁴

¹ Department of Physics, Govt.College for Women (A), Kumbakonam - 612 001, India.

² Department of Physics, Arunai Engineering College, Tiruvannamalai - 606 603, India.

³ Department of Chemistry, Arunai Engineering College, Tiruvannamalai - 606 603, India.

⁴ Department of Physics, Thiru.A.Govindasamy Arts College, Thindivanam- 604 001, India.

ARTICLE INFO

Article history:

Received: 2 December 2016;

Received in revised form:

7 February 2017;

Accepted: 18 February 2017;

Keywords

ZnO,

Capped,

Polyvinylpyrrolidone,

Quantum confinement effect,

Nanorods.

ABSTRACT

ZnO nanorods were successfully fabricated by using the chemical precipitated method. We report the synthesis and characterization of several sizes of ZnO nanocrystals, both in the free standing and the capped particle forms. The sizes of these nanocrystals could be controlled by capping them with polyvinylpyrrolidone and were estimated by X-ray diffraction and transmission electron microscopy. The chemical compositions of the products were characterized by FT-IR spectroscopy. UV -Vis absorption spectroscopy measurements reveal that the capping of ZnO leads to blue shift due to quantum confinement effect. PL emission spectrum of PVP encapsulated ZnO shows red shift due to defect oriented emission. The morphology of the particles was evaluated by scanning electron microscopy (SEM) and Transmission electron microscopy (TEM). Both the thermo gravimetric analysis (TGA) and differential thermal analysis (DTA) curves of the ZnO show that no further weight loss and thermal effect were observed at a temperature of above 510°C.

© 2017 Elixir All rights reserved.

1. Introduction

In the present trend, Zinc Oxide, a wide band gap (Eg~3.37eV) and a large binding energy of 60 meV. II-VI semiconductor has been playing vital role because of its application in UV light emitters, varistors, surface acoustic wave devices, piezo electric transducers, gas sensors and solar cells [1-3]. The optical properties of nanomaterials differ from those bulk materials due to quantum confinement effects [4]. To promote the formation of ZnO nanostructures PVP is frequently used as a templating molecule [5]. Despite, a variety of techniques have been employed for synthesis of ZnO particles, such as sol-gel [6], hydrothermal [7], chemical vapour deposition (CVD) [8], electrophoretic deposition [9], vapour-liquid-solid (VLS) methods [10, 11] and thermal decomposition [12], they need high temperature, high pressure and expensive raw materials, which constrained that they are not suitable for large scale production with a relatively low cost. In this paper we report the synthesis and characterization of ZnO nanocrystals via simple chemical precipitation method. To obtain smaller particles and a good control over size, we have capped ZnO nanocrystals with polyvinylpyrrolidone (PVP). These nanocrystals are characterized using X-Ray Diffractometer (XRD), Fourier Transform Infra Red (FTIR) spectroscopy, Scanning Electron Microscopy (SEM), Transition Electron Microscopy (TEM), UV-Visible absorption spectra, Photoluminescence (PL) emission spectra, and Thermo Gravimetric-Differential Thermal analysis (TG-DTA).

2. Materials and methods

2.1 Materials

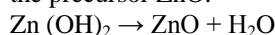
Zinc acetate dihydrate (Zn (CH₃COO)₂ · 2H₂O), sodium hydroxide (NaOH), and Poly-VinylPyrrolidone (PVP mw = 40,000), are purchased from Merck. All chemicals are used as received since they were of analytical reagent grade with 99% purity. The glass wares used in this experimental work were acid washed. Ultrapure water was used for all dilution and samples preparation.

2.2 Synthesis of ZnO nanoparticles

The samples of zinc acetate: NaOH with different concentrations 0.03, 0.04, 0.05, 0.06 and 0.07g were used for the synthesis of ZnO nanoparticles by Chemical precipitation method. From the optical properties of synthesized particles, 0.05g of NaOH in 2.2g of zinc acetate was chosen as optimum concentration. The ZnO nanocrystals were synthesized by gradual mixing the solution of Zn (CH₃COO)₂ · 2H₂O and NaOH under vigorous stirring by magnetic stirrer to form white precipitate. The overall reaction for the synthesis of ZnO can be written as

$$\text{Zn (CH}_3\text{COO)}_2 \cdot 2\text{H}_2\text{O} + 2\text{NaOH} \rightarrow 2\text{NaCH}_3\text{COO} + 2\text{H}_2\text{O} + \text{Zn (OH)}_2$$

The precipitate was collected and rinsed three times with high purity water and ethanol respectively. Subsequently, the washed precipitate was dried at 100° C for two hours to form the precursor ZnO.



2.3 Synthesis of PVP encapsulated ZnO nanoparticle

For the synthesis of PVP encapsulated ZnO, 1gm of PVP dissolved in 100ml of deionized water was mixed with Zinc acetate solution (2.2 gm in 100ml of DIW). After several

mixing, the aqueous solution of NaOH (0.05 gm in 100 ml of DIW) was added drop wise under vigorous stirring to form white precipitate of PVP encapsulated ZnO nanoparticles.

2.4 Characterization technique

X-ray diffraction patterns of the ZnO, and PVP encapsulated ZnO were recorded using an XPERT-PRO diffractometer with a $\text{CuK}\alpha$ radiation ($\lambda = 1.54060\text{\AA}$) under the same conditions. The size was calculated using Debye-Scherrer equation $D = 0.89 \lambda / \beta \cos\theta$ at the half width at a full maximum of the major XRD peaks. The FT-IR studies were carried out using NICOLET AVATAR 360 FT-IR spectrometer. The optical absorption spectra of the samples were recorded using a UV 1650 PCSHIMADZU spectrometer. Size and morphology of the particles were determined using TEM (PHILIPS-CM200; 20-20kv) and scanning electron microscopy (SEM; JEOL- JSM-5610LV). Elemental composition was analyzed using the EDX attachment in the same SEM instrument. Fluorescence measurements were performed on an RF-5301PC spectrometer. Emission spectra were recorded under 245 nm excitation for all samples. Thermo gravimetric –Differential Thermal Analysis was carried out by STD Q600 V 8.3 Build 101 thermal analyzer in nitrogen atmosphere at the rate of $10^\circ\text{C}/\text{min}$.

3. Results and discussion

3.1 Crystal structure and size

The XRD patterns obtained for the free standing ZnO, and PVP encapsulated ZnO nanoparticles are shown in figure 1. In all cases, prominent peaks (101), (100), (002) planes, wurtzite structures of ZnO were detected [13]. Furthermore, it can also be seen that the enhance intensity of (101) peak is dominate over all the peaks conforming the formation of wurtzite structure, this peak is indicative of anisotropic growth and implies a preferred orientation of crystallites. Diffraction peaks related to impurities were not observed in the XRD pattern, confirming the high purity of the synthesized product. Furthermore, it could be noted that the diffraction peaks of PVP encapsulated ZnO nanoparticles were more intense and sharper implying a good crystalline nature of the as synthesized ZnO product [14]. In addition, the broadening at the bottom of diffraction peaks also denotes that the crystalline sizes were small as a result of PVP capping. The average crystalline size (D) of the nanosized particles can be obtained from Debye-Scherrer formula $D = 0.89\lambda / (\beta \cos \theta)$, where D is the crystalline size (in nm), β the full width at half maximum (FWHM- in radian) intensity, and θ the Bragg diffraction angle. The average particle size was estimated at 14.5, and 7.8nm for ZnO, and PVP encapsulated ZnO respectively.

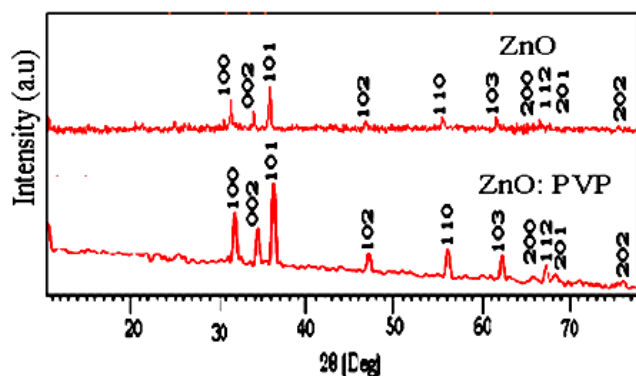


Fig 1. XRD patterns of ZnO and PVP capped ZnO Nanocrystals.

3.2 Functional group analysis

In order to justify the role of PVP in the growth of ZnO nanoparticles, FT-IR spectra of PVP and ZnO nanoparticles

without and with PVP were recorded as shown in figure 2. In the pure ZnO, the broad absorption bands at 3434 and 1636 cm^{-1} are due to O-H stretching and bending vibrations of absorbed water in the ZnO surface. The absorption peak around 2432 cm^{-1} is due to the existence of CO_2 molecules in air.

The strong absorption bands between 550 and 430 cm^{-1} can be attributed to the stretching modes of ZnO [15]. The appearance of absorption band at 464 cm^{-1} explains the morphology dependency of the synthesized ZnO particles as spherical [16].

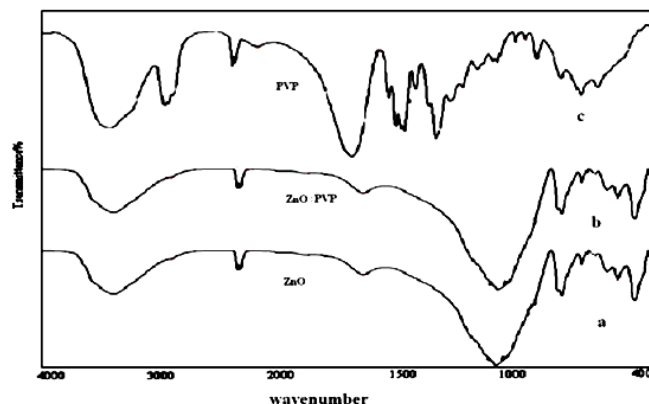


Fig 2. FT-IR Spectra of (a) ZnO (b) ZnO: PVP (c) PVP.

In the spectrum of pure PVP molecule five characteristic absorption peaks located at 3440 , 2956 , 1652 , 1423 , and 1292 cm^{-1} , are assigned to the O-H stretching vibration, CH_2 unsymmetrical stretching vibration, C=O stretching vibration, CH_2 bending vibration and C-N stretching vibration band, respectively. In the spectra of ZnO nanoparticles without and with PVP, they show nearly the same spectra and no peak belonging to PVP is detected as they are completely washed out at the time of synthesis.

3.3 Particle morphology

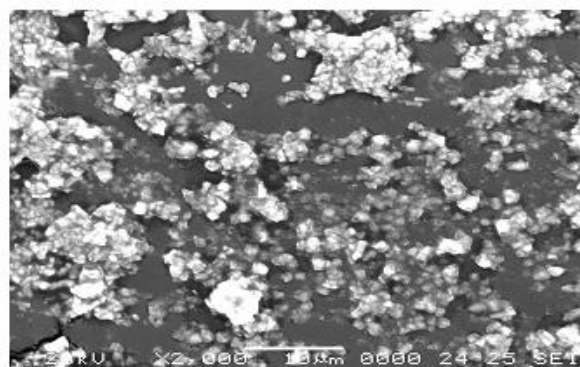


Fig 3. SEM image of ZnO Nanocrystals.

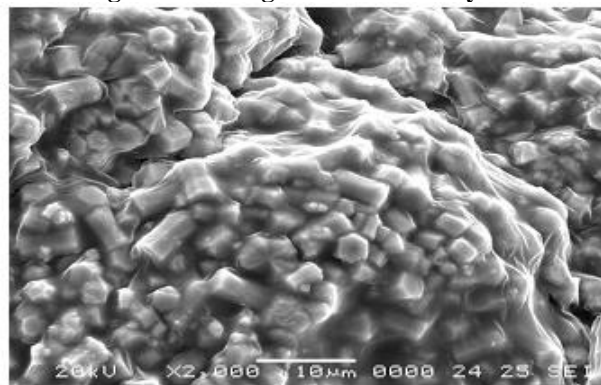


Fig 4. SEM image of PVP encapsulated ZnO Nanocrystals.

The TEM images of ZnO and PVP capped ZnO are shown in figures 5 and 6. From the TEM image of ZnO, it is

clear that the materials appear to be granule particles and many of them agglomerate which indicate the incomplete nucleation growth. In the TEM image of PVP coated ZnO nanoparticles, particles are well separated with no agglomeration. With the introduction of PVP, Zinc ions or particles would coordinate with N or O in PVP, and a covered layer would generate on the surface of the particles. The layer inhibited the growth and agglomeration of the particles [14]. As can be seen from the figure 6, the sample consists of straight and smooth rods.

The diameter and the length of the nanorods are 7-13nm and 32-100nm, respectively. These results are in good agreement with the corresponding XRD data mentioned above.

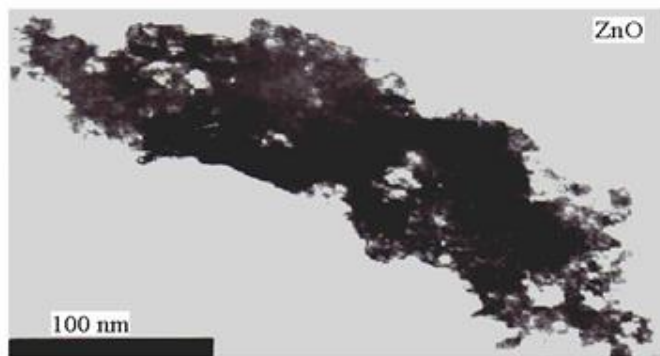


Fig 5. TEM image of ZnO Nanocrystals.

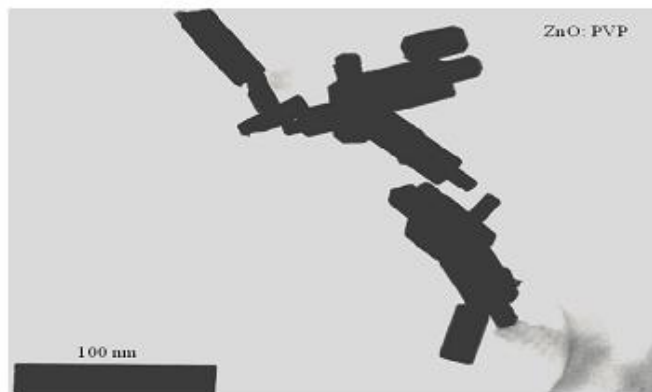


Fig 6. TEM image of PVP encapsulated ZnO Nanocrystals.

3.4 Optical absorption

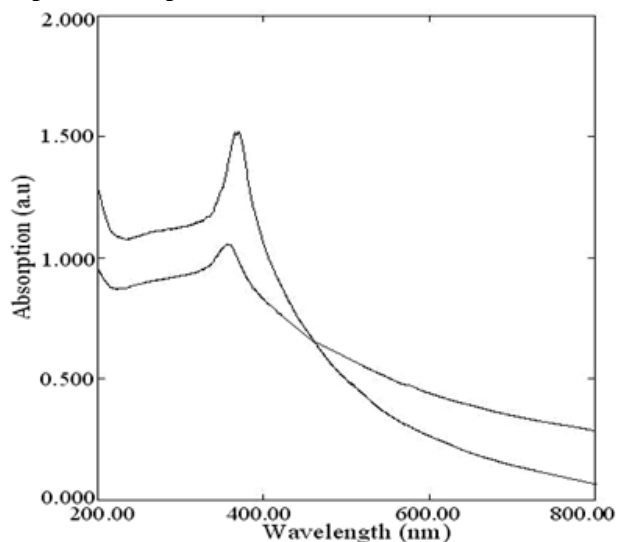


Fig 7. UV –Visible absorption spectra of ZnO and PVP encapsulated ZnO.

Figure 7 shows the absorption spectra of uncapped ZnO, and PVP capped ZnO nanoparticles. The absorption peaks

corresponding to ZnO and PVP capped ZnO are 365, and 345 nm, respectively and the peak position reflects the band gap of the nanoparticles. Compared to ZnO nanoparticles, PVP encapsulated ZnO nanoparticles have significant blue- shifted absorption peak due to the controlled growth of the ZnO particles.

The optical band gaps were calculated and are 3.45eV and 3.62 eV, respectively, for freestanding ZnO and PVP encapsulated ZnO nanoparticles. The obtained values of the band gap of the synthesized nanoparticles are higher than that of the bulk value of ZnO (3.37 eV). This blue shift of the band gap takes place because of the quantum confinement effect [18].

3.5 Photoluminescence properties

The room temperature Photoluminescence (PL) emission spectra of freestanding and PVP encapsulated ZnO nanoparticles with excited wavelength of 245nm are shown in figures 8 and 9. The emission spectrum of ZnO consists of three bands in the visible region: a strong blue band at 433nm, a weak blue band at 466nm, and a weak blue green band at 486nm, whereas no UV band edge emission was observed. The quenching of UV emission is due to presence of surface impurities in ZnO nanoparticles. The blue emission is from Zinc vacancies and Zinc interstitial defects. The weak blue and weak blue green emissions are possibly due to the surface defect in the ZnO powders reported by Wang and Gao [19]. The addition of PVP, the capping agent with ZnO shows the enhancement in red shift. The enhancement in red shift does not mean the decrease in band gap of ZnO but due to defect related radiative recombination [13].

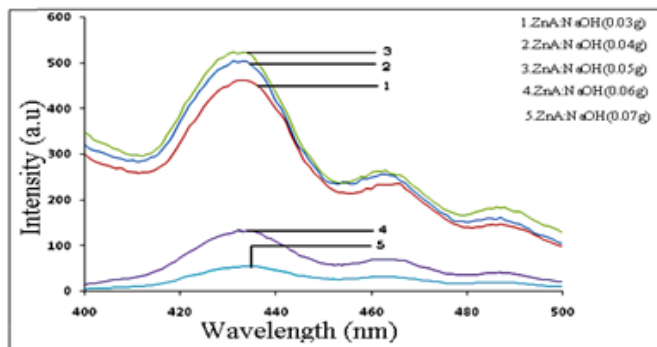


Fig 8. PL spectra of ZnO for different concentrations of NaOH.

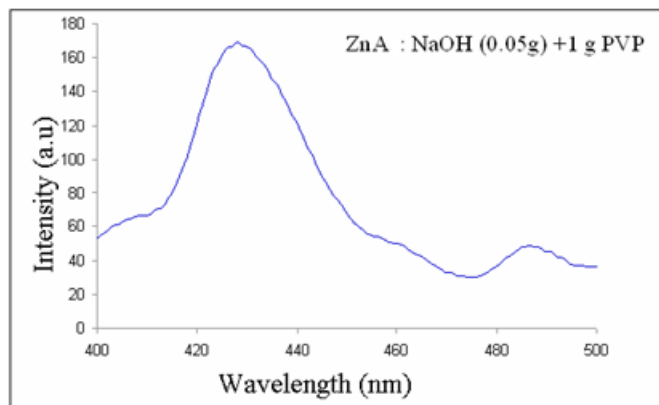


Fig 9. PL spectra of PVP encapsulated ZnO.

3.6 Thermal analysis of ZnO

Figure 10 shows the TG and DTA traces of ZnO which was heated from room temperature to 1200°C at 10°C per min in a nitrogen atmosphere. TGA curve shows that the major

weight loss occurs in the temperature range 250 to 450°C. The weight loss was related to the decomposition of the precursors of ZnO. The sharp plateau formed at a temperature between 450 and 1200°C on the TGA curve indicates that the formation of nanocrystalline ZnO was a decomposition product, as confirmed by XRD analysis [20]. On the DTA curve a major exothermic effect was observed between 320 and 500°C with a maximum at about 385°C, indicating that the thermal events could be associated with the decomposition of the precursors of ZnO. Both no further weight loss and no thermal effect were observed at a temperature of above 510°C, indicating that decomposition does not occur above this temperature and the stable residues are may be ascribed to ZnO nanoparticles.

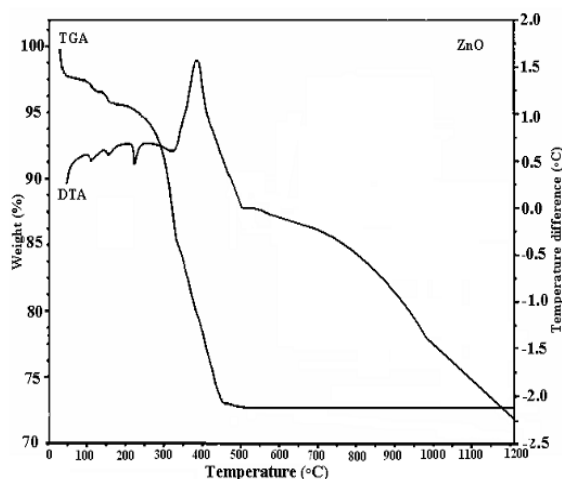


Fig 10. TG-DTA analysis of ZnO Nanocrystals.

4. Conclusions

We have synthesized nanocrystals of pure and PVP encapsulated ZnO through chemical precipitation method. XRD analysis revealed the formation of single phase wurtzite ZnO structure and their nanocrystalline nature. The Scherrer's formula showed the particle sizes are in the range of 14.5nm for pure ZnO and 7.8nm for capped nanoparticles. The FT-IR analysis has confirmed the formation of ZnO. SEM studies showed the transformation of spherical particles into rod shape on PVP capping. It was found that the capped ZnO nanoparticles have a better morphology than the uncapped one and also PVP encapsulation on ZnO decreases the size of the particles. TEM study showed that the synthesized nanorods are perfectly monodispersed. The diameter and the length of the nanorods are 7-13nm and 32-100nm, respectively. The optical absorption showed that UV absorption peak of the capped ZnO was blue shifted compared with bulk ZnO, which clearly indicate the strong quantum confinement. The PL emission peaks were red shifted due to defect oriented emissions. The enhancement in red shift reinforcing the conclusion, that the emission levels are not rigidly connected to the band gap of ZnO. The thermal studies revealed that crystalline ZnO particles are formed at the calcinations temperature of 510°C.

References

[1] Wang, Z.L, M. Chen, Z.L. Pei, C. Sun, L.S. Wen, X. Wang. Surface characterization of transparent conductive oxide Al-doped ZnO films. *J Cryst Growth* 2000; 220(3):254-62.
 [2] G. Socol, D. Craciun, I.N. Mihailescu, N. Stefan, C. Besleaga, L. Ion, S.J. Pearton, et al. High quality amorphous indium zinc oxide thin films synthesized by pulsed laser deposition. *Thin Solid Films* 2011; 520(4):1274-77.

[3] Yuxin Wang, Xinyong Li, Ning Wang, Xie Quan, Yongying Chen. Controllable synthesis of ZnO nanoflowers and their morphology-dependent photocatalytic activities. *Sep Purif Technol* 2008; 62(3):727-32.
 [4] Tao Z, Yu X, Fei X, Liu J, Yang G, Zhao Y, Yang S, Synthesis and photoluminescence of Cl-doped ZnO nanospheres. *Opt Mater* 2008; 31(1):1-5.
 [5] Lepton N, Van Bael Mk, Van den Rul H D, R. Peeters, D. Franco, J. Mullens. Structural and luminescent properties of ZnO nanorods prepared from aqueous solution. *Mater Lett* 2007; 61(13):2624-27.
 [6] Lionel Vayssieres, Karin Keis, Anders Hagfeldt, and Sten-Eric Lindquist. Three- dimensional array of highly oriented crystalline ZnO microtubes. *Chem Mater* 2001; 13(12):4395-4401.
 [7] Hu J.Q, Li Q, Wong N.B, Lee C.S. Synthesis of uniform hexagonal prismatic ZnO Wiskers. *Chem Mater* 2002; 14(3):1216-19.
 [8] Jih-Jen Wu, Sai-Chang Liu. Catalyst-free Growth and characterization of ZnO nanorods. *J Phys Chem B* 2002; 1069(37): 9546-51.
 [9] Yong Eui Lee, David P. Norton, and John D. Budai. Enhanced photoluminescence in epitaxial ZnGa₂O₄: Mn thin-film phosphors using pulsed-laser deposition. *Appl Phys Lett* 1999; 71(2):3155-3157.
 [10] Huang, S, Mao M.H, Yan H, Wu Y, Feick H, Russo R, Yang P. Room- Temperature ultraviolet nanowire nanolasers. *Science/AAAS* 2001; 292:1897- 99.
 [11] Yang P, Yan H, Mao S, Russo R, Jhonson J, Morris N, et al. Controlled growth of ZnO nanowire. *Adv Funct Mater* 2002; 12 (5):323-328.
 [12] Yin M, Gu Y, Kuskovsky I.L, Andelman T, Zhu Y, Neumark G.F, Brien S.O. Zinc oxide quantum rods. *J Am Chem Soc* 2004; 126:6206-6208.
 [13] Sharda, Jayanthi, K, Chawla, Santa. Synthesis of Mn doped ZnO nanoparticles with biocompatible capping. *Appl Surf Sci* 2010; 256(8):630-635.
 [14] Rajeswari Yogamalar N, Srinivas an R, Chandra Bose A. Multi-capping agents in size confinement of ZnO nanostructured particles. *Opt Mater* 2009; 31(11):1570-1574.
 [15] D.M. Fernandes, R. Silvaa, A.A.Winkler Hechenleitner, E. Radovanovic, M.A. Custódio Melo, E.A. Gómez Pineda. Synthesis and characterization of ZnO, CuO and a mixed Zn and Cu oxide. *Mater Chem Phys* 2009; 115(1):110-115.
 [16] The Infrared Spectra Hand book of Inorganic Compounds. Sadtler Research Lab. Heydens son Ltd; London; 1984.p.267- 86.
 [17] Fanfei Bai, Ping He, Zhijie Jia, Xintang Huang, Yun He. Size - controlle preparation of monodispersed ZnO nanorods. *Mater Lett* 2005; 59(13):1687- 90.
 [18] Bhargava R.N and Gallagher D. A novel route to photoluminescent, water-soluble Mn-doped ZnS quantum dots via photopolymerization initiated by the quantum dots. *Phys Rev Lett* 1994; 72(8):416-19.
 [19] Jinmin Wang and Lian Gao. Hydrothermal synthesis and photoluminescence properties of ZnO nanowires. *Solid State Commun* 2004; 132(3-4):269-71.
 [20] Santi Maensiri, Paveena Laokul, Vinich Promarak, Synthesis and optical properties of nanocrystalline ZnO powders by a simple method using zinc acetate dihydrate and poly (vinyl pyrrolidone). *J Cryst Growth* 2006; 289:102-106.